

Non-empirical Study of Superconductivity in Alkali-doped Fullerides Based on Density Functional Theory for Superconductors

Ryosuke Akashi¹ and Ryotaro Arita^{1,2}

¹*Department of Applied Physics, The University of Tokyo, Hongo, Bunkyo-ku, Tokyo 113-8656, Japan and*

²*JST-PRESTO, Kawaguchi, Saitama 332-0012, Japan*

(Dated: June 8, 2021)

We apply the density functional theory for superconductors (SCDFT) based on the local-density approximation (LDA) to alkali-doped fullerides A_3C_{60} with the face-centered cubic structure. We evaluate the superconducting transition temperature (T_c) from first principles considering energy dependence of electron-phonon coupling, the mass renormalization, and the retardation effect. The calculated $T_c=7.5$, 9.0 and 15.7 K for $A=K$, Rb, Cs are approximately 60 % smaller than the experimentally observed values. Our results strongly suggest necessity to go beyond the framework of the Migdal-Eliashberg theory based on the LDA.

PACS numbers:

-Introduction. The doped fulleride superconductors A_3C_{60} (A =alkali metal) [1, 2], which exhibit maximum transition temperature (T_c) of 40 K, have provided a fertile playground for theoretical and experimental studies. The most significant feature of the fullerides is the narrow metallic bands formed by molecular orbitals, whose energy scale compete with the vibrational frequencies and electron-electron interactions. Moreover, recent experiments revealed that the T_c -volume (V) curve for this series shows a dome-like dependence near the superconductor-Mott insulator transition [3–7]. This dependence is, similarly to the celebrated superconducting dome in cuprates, reminiscent of a crossover from weak to strong correlation in this system.

Motivated by these properties, various theoretical studies have investigated unconventional pairing mechanisms [1, 8]. On the other hand, there have also been a received idea that the superconductivity in this system is explained by the conventional phonon-mediated pairing mechanism. Full s-wave gap with spin-singlet pairing [9–11], C-isotope effect coefficient of $\gtrsim 0.20$ [12–14], and the coherence peak in the NMR and μ SR relaxation rate [15, 16] have been experimentally observed. In particular, in the T_c - V plot, the regime where T_c and V positively correlate is seemingly consistent with the BCS theory; increasing V results in smaller bandwidths, larger density of states (DOS) at the Fermi level, and subsequently stronger electron-phonon coupling. Hence, the applicability of the phonon mechanism is still unsettled.

The Migdal-Eliashberg (ME) theory [17], which is a quite widely applicable theory of phonon-mediated superconductivity, includes the self energy with the lowest-order exchange contribution of the dressed phonons and the static screened Coulomb interaction. The ME theory described by the Kohn-Sham orbital based on the local-density approximation [18, 19] (KS-LDA) has enabled us to consider fine details of materials [20–22]. Moreover, the recently developed density functional theory for superconductors (SCDFT) [23, 24] has provided us a way to

calculate T_c based on the ME theory nonempirically. The SCDFT treats effects of the interactions such as the mass-renormalization [17] and the retardation effect [25] taking the detail of the electronic structure. The T_c calculated with the SCDFT has shown remarkably good agreement with experimentally observed T_c [24, 26, 27]. However, its applications to molecular solids has not been reported due to its expensive computational cost. In this paper, we apply the SCDFT to fcc A_3C_{60} [$A=K$ and Rb under ambient pressure ($T_c=19$ and 29 K), and Cs under the optimum pressure of 7 kbar ($T_c=35$ K)] focusing on the regime where T_c and V positively correlate. We calculate T_c to see if the SCDFT reproduces the absolute values and the alkali-metal dependence of the experimentally observed T_c , with which we examine the applicability of the ME theory with the KS-LDA in the present system. The calculated T_c suggests that we need to consider some factors missing in the framework of the ME theory based on the KS-LDA.

-Method. In the current SCDFT [23, 24] we solve the gap equation given by

$$\Delta_{n\mathbf{k}} = -Z_{n\mathbf{k}}\Delta_{n\mathbf{k}} - \frac{1}{2} \sum_{n'\mathbf{k}'} \mathcal{K}_{n\mathbf{k}n'\mathbf{k}'} \frac{\tanh[(\beta/2)E_{n'\mathbf{k}'}]}{E_{n'\mathbf{k}'}} \Delta_{n'\mathbf{k}'}. \quad (1)$$

Here, n and \mathbf{k} denote the band index and crystal momentum, respectively, Δ is the gap function, and β is the inverse temperature. The energy $E_{n\mathbf{k}}$ is defined as $E_{n\mathbf{k}} = \sqrt{\xi_{n\mathbf{k}}^2 + \Delta_{n\mathbf{k}}^2}$ and $\xi_{n\mathbf{k}} = \epsilon_{n\mathbf{k}} - \mu$ is the one-electron energy measured from the chemical potential μ , where $\epsilon_{n\mathbf{k}}$ is obtained by solving the normal Kohn-Sham equation $\mathcal{H}_{\text{KS}}|\varphi_{n\mathbf{k}}\rangle = \epsilon_{n\mathbf{k}}|\varphi_{n\mathbf{k}}\rangle$ with \mathcal{H}_{KS} and $|\varphi_{n\mathbf{k}}\rangle$ being the Kohn-Sham Hamiltonian and the Bloch state, respectively. The functions Z and \mathcal{K} are the exchange-correlation kernels describing the effects of the interactions. The kernels describing the standard electron-phonon mechanism, $\mathcal{K}=\mathcal{K}^{\text{ph}}+\mathcal{K}^{\text{el}}$ and $Z=Z^{\text{ph}}$, have been proposed [23, 24]. Namely, the phonon contributions (\mathcal{K}^{ph} and Z^{ph}) were formulated referring to the ME theory, and the electron contribution (\mathcal{K}^{el}) corresponds to

the screened static Coulomb interaction scattering the Cooper pairs.

Since the fulleride superconductors involve high-frequency phonons, the electron-phonon interaction has strong dependence on both $\xi_{n\mathbf{k}}$ and $\xi_{n'\mathbf{k}'}$. In order to treat this effect, we use the $n\mathbf{k}$ -resolved form for \mathcal{K}^{ph} and \mathcal{Z}^{ph} defined by Eqs. (9) and (11) in Ref. 24, which require the electron-phonon matrix elements $g_{n\mathbf{k},n'\mathbf{k}'}^{\nu\mathbf{q}}$ and the phonon frequencies $\omega_{\nu\mathbf{q}}$ as inputs. For \mathcal{K}^{el} , on the other hand, we use the form given by Eq. (13) in Ref. 29, which is based on the static random-phase approximation (RPA) [28] and properly treats the local-field effect due to the spatial dependence of electron density.

-Result and discussion. We calculated the band structure, phonon frequencies, electron-phonon and electron-electron interactions, and T_c for fcc $A_3\text{C}_{60}$ with $A=\text{K}, \text{Rb}$ and Cs . All of our calculations were performed within the local-density approximation using *ab initio* plane-wave pseudopotential calculation codes QUANTUM ESPRESSO [30–32]. Input structural parameters [36] were determined by full relaxation and the Murnaghan equation of state [37]. For $A=\text{Cs}$, we considered the case of the optimum pressure of 7 kbar [7]. Phonon frequency and electron-phonon coupling [38] were calculated by the density functional perturbation theory [39]. The dielectric function used for \mathcal{K}^{el} was calculated within the static RPA. The SCDFT gap equation [Eq. (1)] was solved with the random sampling scheme given in Ref. 40, with which the sampling error in the calculated T_c was approximately 3%.

Let us start from the calculated DOS of the partially occupied t_{1u} bands in Fig. 1. The general trend is consistent with the previous calculation based on the generalized gradient approximation and the experimental lattice constants [42]. As anticipated previously [3, 4], replac-

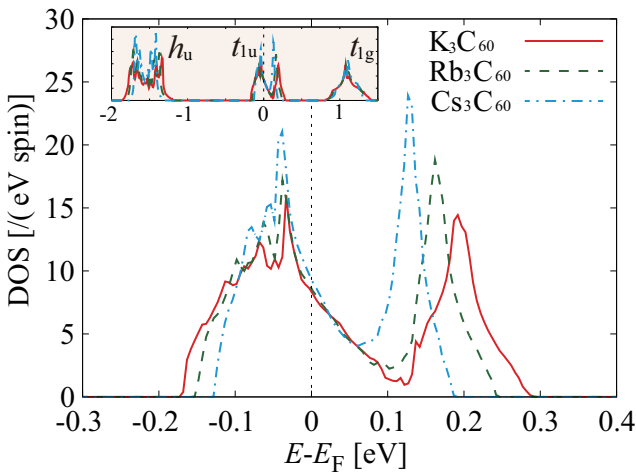


FIG. 1: (Color online) DOS around the Fermi level. Inset is the view in a broader energy scale, where the characters of the bands are specified.

ing lighter alkali metal elements with heavier ones (from K, Rb to Cs) leads to slightly larger DOS at the Fermi level $N(0)$ (see Table I). More significantly, we also see that the bandwidth becomes narrower. The relation between these changes and the electron-phonon coupling is discussed later.

Table II summarizes our calculated frequencies of the Γ -point H_g -derived modes, which are distinguished as five-fold degenerate branches with strong electron-phonon coupling. The experimentally observed and preceding theoretical frequencies are also given for comparison. The agreement between our calculation and experiments is extremely good, which illustrates that our calculation properly describes the phonon properties of the present system. The alkali-metal dependence of the frequencies is little, which is due to the intramolecular property of the modes.

We next show the T_c calculated by the SCDFT with only the phonon contributions to the gap-equation kernels (\mathcal{K}^{ph} and \mathcal{Z}^{ph}). The calculated T_c (red solid square) is higher than the experimental T_c , which is because of the absence of the electron contribution. These values are consistent with the recent calculation based on the Eliashberg equation [17] by Koretsune and Saito [47]. Interestingly, the experimentally observed alkali-metal dependence is reproduced. In order to examine the origin of this dependence, we calculated the electron-phonon coupling coefficient $\lambda_{N(0)} = \frac{2}{N(0)} \sum_{\mathbf{k}\mathbf{q}n\nu} \frac{|g_{n'\mathbf{k}+\mathbf{q},n\mathbf{k}}^{\nu\mathbf{q}}|^2}{\omega_{\nu\mathbf{q}}} \delta(\xi_{n\mathbf{k}}) \delta(\xi_{n'\mathbf{k}+\mathbf{q}})$ and the characteristic frequency $\omega_{\text{ln},N(0)} = \exp \left\{ \frac{2}{N(0)\lambda_{N(0)}} \sum_{\mathbf{k}\mathbf{q}n\nu} \frac{|g_{n'\mathbf{k}+\mathbf{q},n\mathbf{k}}^{\nu\mathbf{q}}|^2}{\omega_{\nu\mathbf{q}}} \delta(\xi_{n\mathbf{k}}) \delta(\xi_{n'\mathbf{k}+\mathbf{q}}) \ln \omega_{\nu\mathbf{q}} \right\}$. The calculated values are listed in Table I. By replacing lighter alkali-metal elements with heavier ones, $\lambda_{N(0)}$ is slightly enhanced due to the increase of $N(0)$. However, when we substitute $\lambda_{N(0)}$ and $\omega_{\text{ln},N(0)}$ into the McMillan-Allen-Dynes (MAD) formula [48], $T_c = \frac{\omega_{\text{ln}}}{1.2} \exp[-1.04(1 + \lambda)/\lambda]$ (with the Coulomb pseudopotential μ^* set to 0), the dependence of the resulting T_c (blue open circle) is not as significant as that obtained from the SCDFT. Alternatively, we calculated $\lambda_{N(\xi)}$ and $\omega_{\text{ln},N(\xi)}$ defined by the

TABLE I: Calculated parameters representing the electronic structure and the electron-phonon and electron-electron interactions.

	K_3C_{60}	Rb_3C_{60}	Cs_3C_{60}
$N(0)$ [/(eV spin)]	8.352	8.609	9.328
$\lambda_{N(0)}$	0.562	0.570	0.603
$\lambda_{N(\xi)}$	0.489	0.542	0.652
$\omega_{\text{ln},N(0)}$ [K]	1071	1054	1052
$\omega_{\text{ln},N(\xi)}$ [K]	932	944	940
\mathcal{Z}	0.350	0.367	0.396
μ	0.379	0.370	0.362

TABLE II: Experimentally observed and theoretically calculated Γ -point phonon frequencies (cm^{-1}). The dashes denote the splitting induced by the crystal field.

	expt.		present			theory	
	^a C ₆₀	^b K ₃ C ₆₀	K ₃ C ₆₀	Rb ₃ C ₆₀	Cs ₃ C ₆₀	^c K ₃ C ₆₀	^d K ₃ C ₆₀
$H_g(1)$	273	271	262–271	261–269	261–270	281	252–258
$H_g(2)$	437	431	422–422	420–422	418–421	454	407–404
$H_g(3)$	710	723	685–689	686–688	687–689	753	658–663
$H_g(4)$	774	. . .	779–779	779–780	779–783	785	737–740
$H_g(5)$	1099	. . .	1111–1116	1111–1116	1113–1120	1091	1019–1023
$H_g(6)$	1250	. . .	1268–1274	1268–1273	1271–1275	1290	1137–1136
$H_g(7)$	1428	1408	1403–1408	1402–1405	1406–1407	1387	1349–1348
$H_g(8)$	1575	1547	1532–1537	1532–1536	1532–1538	1462	1532–1530

^a Raman scattering measurement, Ref. 43.

^b Raman scattering measurement, Ref. 44.

^c *Ab initio* LDA full-potential calculation based on linearized muffin-tin orbital method, Ref. 45.

^d *Ab initio* LDA pseudopotential calculation based on the mixed basis method, Ref. 46.

following formulae [49, 50]

$$\lambda_{N(\xi)} = \frac{2}{N(0)} \sum_{\mathbf{k}\mathbf{q}} \frac{|g_{n'\mathbf{k}+\mathbf{q},n\mathbf{k}}^{\nu\mathbf{q}}|^2}{\omega_{\nu\mathbf{q}}^2} [f_{\beta}(\xi_{n\mathbf{k}}) - f_{\beta}(\xi_{n'\mathbf{k}} + \omega_{\nu\mathbf{q}})] \times \delta(\xi_{n'\mathbf{k}+\mathbf{q}} - \xi_{n\mathbf{k}} - \omega_{\nu\mathbf{q}}) \quad (2)$$

$$\omega_{\ln,N(\xi)} = \exp \left\{ \frac{2}{N(0)\lambda_{N(\xi)}} \sum_{\mathbf{k}\mathbf{q}} \frac{|g_{n'\mathbf{k}+\mathbf{q},n\mathbf{k}}^{\nu\mathbf{q}}|^2}{\omega_{\nu\mathbf{q}}^2} [f_{\beta}(\xi_{n\mathbf{k}}) - f_{\beta}(\xi_{n'\mathbf{k}} + \omega_{\nu\mathbf{q}})] \times \delta(\xi_{n'\mathbf{k}+\mathbf{q}} - \xi_{n\mathbf{k}} - \omega_{\nu\mathbf{q}}) \ln \omega_{\nu\mathbf{q}} \right\}. \quad (3)$$

These formulae explicitly treat the energy conservation in electron-phonon scattering, and therefore include the effects of the electronic states within the phonon energy scale; since the scattering involves energy exchanges of order $\lesssim 0.2$ eV, electronic states within this energy range should contribute to the pair formation. As a result, the

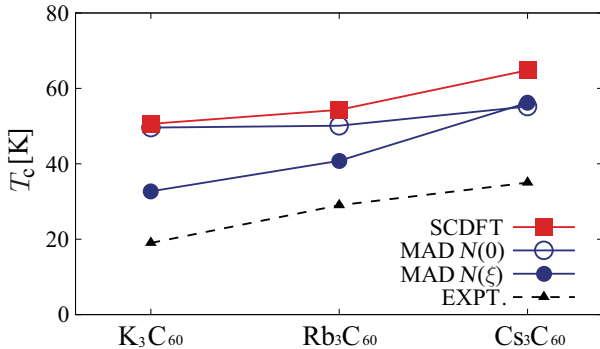


FIG. 2: (Color online) Calculated T_c s: Solid squares denote the values calculated using the SCDFT gap equation with only the phonon contribution (\mathcal{K}^{ph} and \mathcal{Z}^{ph}), and open (solid) circles denote the values derived from the MAD formula (see text) using $\lambda_{N(0)}$ ($\lambda_{N(\xi)}$) and $\omega_{\ln,N(0)}$ ($\omega_{\ln,N(\xi)}$) in Table I. The triangles represent the experimentally observed values.

dependence of the calculated $\lambda_{N(\xi)}$ is more noticeable than that of $\lambda_{N(0)}$, and the corresponding T_c derived from the MAD formula (blue solid circle) well reproduces the dependence of the T_c calculated by the SCDFT and the experimentally observed T_c . The present analysis clarifies the significance of the electronic states within the finite energy range, not only at the Fermi level.

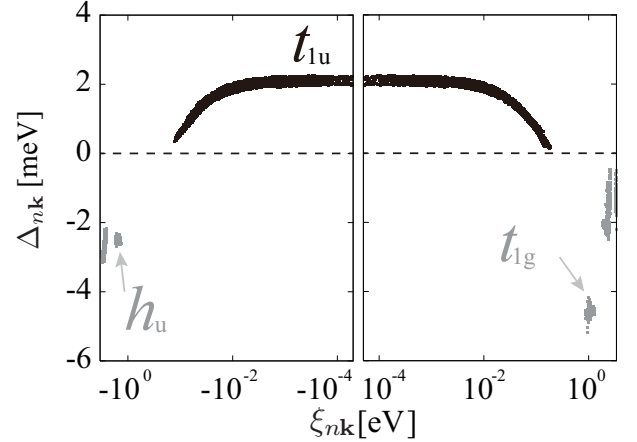


FIG. 3: (Color online) Calculated gap function for Cs₃C₆₀ under pressure of 7 kbar with $T=0.01$ K. The characters of the three bands are specified.

We also found an important aspect of the mass-renormalization factor $\mathcal{Z} \equiv \mathcal{Z}_{n\mathbf{k}}^{\text{ph}}|_{\xi_{n\mathbf{k}} \rightarrow 0}$ given in Table I. In usual cases, \mathcal{Z} is as large as $\lambda_{N(0)}$ [24], but our calculated \mathcal{Z} is much smaller than $\lambda_{N(0)}$ or $\lambda_{N(\xi)}$. This is because that the t_{1u} bands are energetically isolated from other bands. The main contribution to the mass renormalization around the Fermi level generally comes from electron scattering to the states distributed within the several times of the Debye frequency. In the present case, however, the energy scale of the Debye frequency is as large as the bandwidth of the t_{1u} bands, and there is no scattering channel in the gapped region (see the in-

set of Fig. 1). This weak mass renormalization results in relatively higher T_c than expected from the conventional calculations [17, 48].

Next let us move on to the results obtained with the electron contribution (\mathcal{K}^{el}). The strength of \mathcal{K}^{el} is represented by its Fermi-surface average $\mu = \frac{1}{N(0)} \sum_{n\mathbf{k}n'\mathbf{k}'} \mathcal{K}_{n\mathbf{k}n'\mathbf{k}'}^{\text{el}} \delta(\xi_{n\mathbf{k}}) \delta(\xi_{n'\mathbf{k}'})$ (See Table I). We display in Fig. 3 the gap function in $T=0.01\text{K}$ for $A=\text{Cs}$ under pressure of 7 kbar. The values of the gap function in the t_{1u} states are positive, whereas those in the highest doubly occupied h_u and the lowest unoccupied t_{1g} have negative sign. Such sign inversion of the gap function in the high energy region represents the retardation effect in the SCDFT [24]. Here, the absolute values in the high energy region are quite comparable to those in the low-energy region, which signifies the strong retardation effect compared with the previously reported conventional cases [24, 26, 27]. This is due to large interband electron-electron Coulomb interaction.

Finally, we show the calculated T_c for $A=\text{K}$, Rb , and Cs in Fig. 4 together with the experimentally observed T_c . Thanks to the energy dependence of electron-phonon coupling, the alkali-metal dependence of the experimentally observed T_c is well reproduced. In spite of the weak mass renormalization and the significant retardation effect, the absolute values are 7.5, 9.0 and 15.7 K, which are approximately 60% lower than the experimentally observed T_c (19, 29 and 35 K). The present underestimation is in clear contrast with the previous applications to the conventional superconductors [24, 26, 27].

Since the phonon frequency scale in the present system is quite large, the theoretical T_c is sensitive to the input interactions. In fact, with $|g_{n\mathbf{k},n'\mathbf{k}'}^{\nu\mathbf{q}}|^2$ multiplied by 1.2 (0.8), we obtain $T_c=17.5$ (1.5), 20.6 (2.3), and 31.7 (5.0) K for $A=\text{K}$, Rb and Cs , whereas we obtain $T_c=5.8$ (9.6), 7.7 (11.3), 14.7 (18.0) with \mathcal{K}^{el} multiplied by 1.2 (0.8). Concerning the *ab initio* calculation of the interactions, on the other hand, a recent paper reported that the electron-phonon interaction is enhanced by approxi-

mately 30 % by increasing the exchange contribution in the self-consistent calculation of the wavefunctions [51]. These facts imply a possibility to fill the discrepancy between our results and experiments by considering the features neglected in the present ME theory based on the KS-LDA.

-Summary and conclusion. Using the SCDFT, we performed non-empirical calculations of T_c in fcc $A_3\text{C}_{60}$ ($A=\text{K}$, Rb , Cs). We focused on the energy dependence of electron-phonon coupling, the weak mass renormalization and the strong retardation effect. Our calculated values of T_c were 7.5, 9.0 and 15.7 K for $A=\text{K}$, Rb and Cs (under pressure of 7 kbar), which are approximately 60% smaller than the experimentally observed values (19, 29 and 35 K). The present results indicate a necessity to go beyond the ME theory based on the KS-LDA even for the regime where T_c and V positively correlate.

-Acknowledgment. The authors thank Takashi Koretsune and Susumu Saito for fruitful discussions. This work was supported by Funding Program for World-Leading Innovative R&D on Science and Technology (FIRST program) on “Quantum Science on Strong Correlation”, JST-PRESTO, Grants-in-Aid for Scientific Research (23340095) and the Next Generation Super Computing Project and Nanoscience Program from MEXT, Japan.

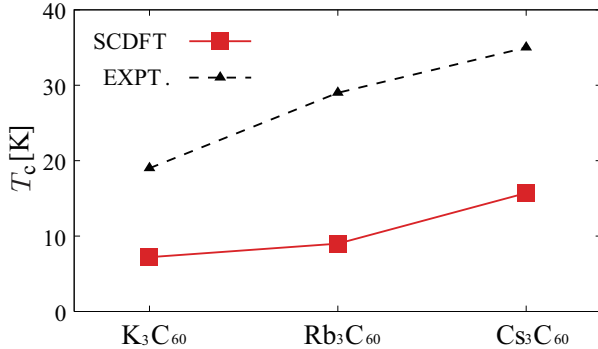


FIG. 4: (Color online) Calculated T_c by solving the SCDFT gap equation with the electron contribution \mathcal{K}^{el} compared with the experimentally observed values.

- [1] O. Gunnarsson, *Alkali-doped Fullerenes: Narrow-band Solids with Unusual Properties*, (World Scientific Publishing Co. Pte, Ltd., Singapore, 2004).
- [2] O. Gunnarsson, Rev. Mod. Phys. **69**, 575 (1997).
- [3] K. Tanigaki *et al.*, Nature **352**, 222 (1991).
- [4] R. M. Fleming *et al.*, Nature **352**, 787 (1991).
- [5] A. Y. Ganin *et al.*, Nat. Mater. **7**, 367 (2008).
- [6] Y. Takabayashi *et al.*, Science **323**, 1585 (2009).
- [7] A. Y. Ganin *et al.*, Nature **466**, 221 (2010).
- [8] M. Capone *et al.*, Rev. Mod. Phys. **81**, 943 (2009).
- [9] Z. Zhang *et al.*, Nature **353**, 333 (1991).
- [10] R. Tycko *et al.*, Phys. Rev. Lett. **68**, 1912 (1992).
- [11] L. Degiorgi *et al.*, Nature **369**, 541 (1994).
- [12] T. W. Ebbesen *et al.*, Nature **355**, 620 (1992).
- [13] C. C. Chen and C. M. Lieber, Science **259**, 655 (1993).
- [14] M. S. Fuhrer *et al.*, Phys. Rev. Lett. **83**, 404 (1999).
- [15] A. Stenger *et al.*, Phys. Rev. Lett. **74**, 1649 (1995).
- [16] R. F. Kiefl *et al.*, Phys. Rev. Lett. **70**, 3987 (1993).
- [17] A. B. Migdal, Sov. Phys. JETP **7**, 996 (1958); G. M. Eliashberg, Sov. Phys. JETP **11**, 696 (1960); D. J. Scalapino, in *Superconductivity* edited by R. D. Parks, (Marcel Dekker, New York, 1969) VOLUME 1; J. R. Schrieffer, *Theory of superconductivity; Revised Printing*, (Westview Press, Colorado, 1971).
- [18] D. M. Ceperley and B. J. Alder, Phys. Rev. Lett. **45**, 566 (1980).
- [19] J. P. Perdew and A. Zunger, Phys. Rev. B **23**, 5048 (1981).
- [20] S. Y. Savrasov and D. Y. Savrasov, Phys. Rev. B **54**, 16487 (1996).

- [21] H. J. Choi *et al.*, Nature **418**, 758 (2002); H. J. Choi *et al.*, Phys. Rev. B **66**, 020513(R) (2002).
- [22] E. R. Margine and F. Giustino, Phys. Rev. B **87**, 024545 (2013).
- [23] M. Lüders *et al.*, Phys. Rev. B **72**, 024545 (2005).
- [24] M. A. L. Marques *et al.*, Phys. Rev. B **72**, 024546 (2005).
- [25] P. Morel and P. W. Anderson, Phys. Rev. **125**, 1263 (1962); N. N. Bogoliubov, V. V. Tolmachev, and D. V. Shirkov, *A New Method in the Theory of Superconductivity* (1958) (translated from Russian: Consultants Bureau, Inc., New York, 1959).
- [26] A. Floris *et al.*, Phys. Rev. Lett. **94**, 037004 (2005).
- [27] A. Sanna *et al.*, Phys. Rev. B **75**, 020511(R) (2007).
- [28] M. S. Hybertsen and S. G. Louie, Phys. Rev. B **35**, 5585 (1987); M. S. Hybertsen and S. G. Louie, *ibid.* **35**, 5602 (1987).
- [29] S. Massidda *et al.*, Supercond. Sci. Technol. **22**, 034006 (2009).
- [30] P. Giannozzi, *et al.*, J. Phys.: Condens. Matter **21**, 395502 (2009); <http://www.quantum-espresso.org/>.
- [31] N. Troullier and J. L. Martins, Phys. Rev. B **43**, 1993 (1991).
- [32] The pseudopotential for C was generated in the configuration of $(2s)^{2.0}(2p)^{2.0}$, whereas those of K, Rb, and Cs were generated in the ionized configurations of $(3p)^{6.0}(4s)^{0.0}(3d)^{0.0}$, $(4p)^{6.0}(5s)^{0.0}(4d)^{0.0}$, and $(5p)^{6.0}(6s)^{0.0}(5d)^{0.0}$ with the partial core correction [33]. The plane-wave energy cutoff was set to 50 Ry. The charge density was calculated with the $4\times 4\times 4$ k points in the Monkhorst-Pack grid. The dynamical matrices were calculated on the $2\times 2\times 2$ q points, where the gaussian of width 0.025 Ry was used for the Fermi-surface integration. The electron-phonon matrix elements were calculated on the $(4\times 4\times 4)\times(2\times 2\times 2)$ $k\times q$ points. Using the output of PW code, the electron dielectric function ϵ was calculated on the $3\times 3\times 3$ q points from the Bloch states on the $3\times 3\times 3$ k points using the tetrahedron linear interpolation [34] with the Rath-Freeman treatment [35] considering 129 doubly occupied, 3 partially occupied, and 218 unoccupied bands. The SCDFEFT gap equation was solved with 6000 k points for the t_{1u} bands and 100 points for the other bands, where we considered 129 doubly occupied, 3 partially occupied, and 218 unoccupied bands. We found that, with the tetrahedron interpolation, the convergence of the calculated electronic DOS within order of 0.1 / (eV spin) is achieved by $16\times 16\times 16$ k points. Hence, we used the energy eigenvalues of the t_{1u} states on a supplementary $15\times 15\times 15$ k points for the calculation of the dielectric function, and generated the sampling points for solving the gap equation from the energy eigenvalues on $17\times 17\times 17$ k points.
- [33] S. G. Louie, S. Froyen, and M. L. Cohen, Phys. Rev. B **26**, 1738 (1982).
- [34] G. Lehmann and M. Taut, Phys. Stat. Sol. **54**, 469 (1972).
- [35] J. Rath and A. J. Freeman, Phys. Rev. B **11**, 2109 (1975).
- [36] With ignoring the orientational disorder of the C_{60} molecules, we calculated relaxed lattice constants and internal parameters for $A=K$ and Rb. For $A=Cs$ under pressure of 7kbar, we optimized the atomic configurations for different lattice constants and subsequently derived the corresponding lattice constant from the Murnaghan equation of state [37]. The calculated (experimental [7, 41]) lattice constants were 14.208 (14.240, room temperature), 14.404 (14.420, room temperature), 14.740 (14.500, $T=15$ K) Å for $A=K$, Rb, Cs (7kbar). The relaxed bond lengths of the pentagonal and hexagonal edges, which did not show significant alkali-metal and orientational dependence, were ~ 1.43 and ~ 1.40 Å, respectively.
- [37] F. D. Murnaghan, **30**, 244 (1944).
- [38] We calculated the electron-phonon matrix elements $g_{n\mathbf{k},n'\mathbf{k}'}^{\nu\mathbf{q}}$ only for the three partially occupied t_{1u} bands. Also, we omitted the contribution from the lowest 9 phonon branches, some of which show imaginary frequencies in the present accuracy. These 9 branches are formed by the acoustic modes, librations and independent vibration of alkali-metal atoms in octahedral sites.
- [39] S. Baroni *et al.*, Rev. Mod. Phys. **73**, 515(2001).
- [40] R. Akashi *et al.*, Phys. Rev. B **86**, 054513 (2012).
- [41] O. Zhou and D. E. Cox, J. Phys. Chem. Solids **53**, 1373 (1992).
- [42] Y. Nomura, K. Nakamura, and R. Arita, Phys. Rev. B **85**, 155452 (2012).
- [43] D. S. Bethune *et al.*, Chem. Phys. Lett. **179**, 181 (1991).
- [44] P. Zhou *et al.*, Phys. Rev. B **45**, 10838 (1992).
- [45] V. P. Antropov, O. Gunnarsson, and A. I. Liechtenstein, Phys. Rev. B **48**, 7651 (1993).
- [46] K. P. Bohnen *et al.*, Phys. Rev. B **51**, 5805 (1995).
- [47] T. Koretsune and S. Saito, private communication.
- [48] P. B. Allen and R. C. Dynes, Phys. Rev. B **12**, 905 (1975).
- [49] P. B. Allen, Phys. Rev. B **6**, 2577 (1972).
- [50] M. Casula *et al.*, Phys. Rev. Lett. **107**, 137006 (2011).
- [51] J. Laflamme Janssen *et al.*, Phys. Rev. B **81**, 073106 (2010).